INDIVIDUALLY ADDRESSABLE, 3D-PRINTED CARBON NANOTUBE FIELD EMITTER ARRAYS FOR LARGE-AREA VACUUM ELECTRONICS

Crystal E. Owens, Alex Kachkine*, Gareth H. McKinley, Luis F. Velásquez-García, and A. John Hart*
*These authors contributed equally to this work
Massachusetts Institute of Technology, Cambridge, MA, USA

ABSTRACT

We report the design, fabrication, and characterization of the first known 3D-printed, individually addressable field emitter arrays (FEAs), created via direct deposition of a made-for-purpose carbon nanotube (CNT) ink. The array fabrication is maskless yet automated, rapid (<2 minutes), inexpensive (≪$0.01 per emitter material cost), and produces substantially less waste than traditional subtractive manufacturing methods. Resulting CNT FEAs have tip current density above 10^6 A/cm^2, array current density over 100 mA/cm^2, and field enhancement factors over 10^5 cm^{-1}, matching state-of-the-art CNT-based counterparts. Our approach unlocks the potential for large area (meter scale), individually addressable FEAs, with great relevance to electron projection lithography (EPL), radars, displays, medical imaging, and other vacuum microelectronics applications.

KEYWORDS

3D printing, additive manufacturing, carbon nanotubes, cathodes, field emission, vacuum electronics

INTRODUCTION

Compared to mainstream thermionic cathodes, CNT-based field emission electron sources consume less power and tolerate poorer (>10^{-7} Torr), reactive vacuum [1],[2]. Although cleanroom-microfabricated FEAs attain high performance, their manufacturing is costly, time consuming, and environmentally detrimental due to etchants typically used and their waste products; moreover, the area of a monolithic FEA is limited by the size of the wafers employed [3],[4]. CNTs are favored for field emission over many other materials due to characteristic low power needs and outstanding electron transport properties of the nanotubes. However, CNT-based FEAs have required manual assembly of individually-produced emitters [3], dramatically limiting scalability, or otherwise rely on methods of manufacture that prevent individual addressability, such as weaving long fibers or spincoating CNT inks over an area. These factors hinder use of FEAs in large-area applications, especially when externally programmed electric field compensation is required for uniform array operation, *e.g.*, EPL [5].

Additive manufacturing (AM) can address these limitations by enabling customized material deposition on arbitrary substrates in ambient conditions. Existing literature has reported AM of individual, free-standing CNT emitters [4] and planar, 2D CNT traces [6], [7]; expansion to individually addressable, multi-emitter arrays is required for many applications yet has not been achieved due in part to process challenges of material handling and alignment of emitters into regular arrays. The need for this development and resulting devices is apparent in industry. For instance, low-cost FEAs hold great utility for healthcare, potentially enabling phase contrast X-ray imaging of soft tissue without contrast media [8].

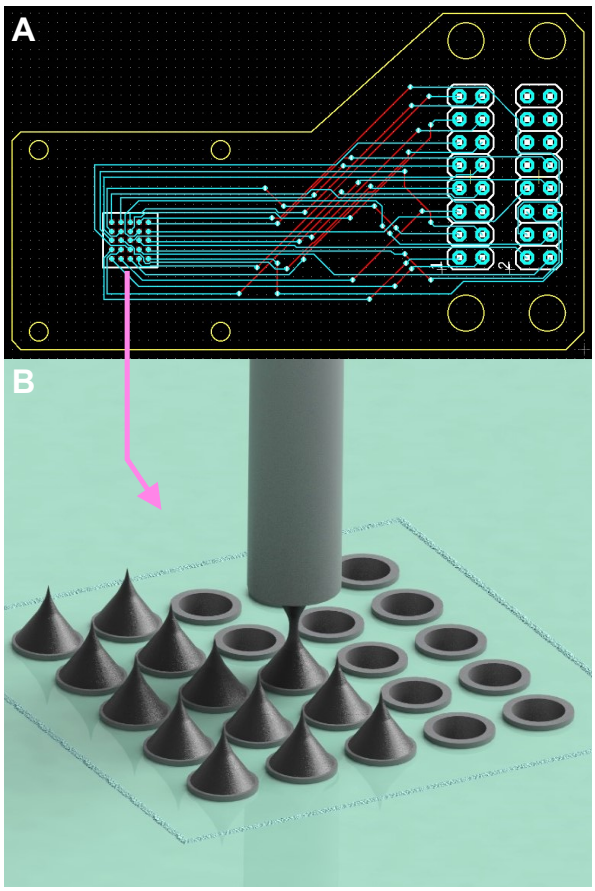

Figure 1: Printing of arrays of individually addressable field emitters. A) PCB wiring schematic. B) Rendering of point-by-point printing process from cylindrical printing nozzle; each emitter is extruded on top of a different PCB vias, yielding an array of individually addressable field emitters.

METHODS

Device Design

The proof-of-concept FEAs comprise 5 by 5 arrays of 1 mm-spaced CNT ink aliquots extruded on copper vias of a bespoke PCB individually addressed with 127 µm copper traces (Figure 1). The CNT deposition was performed using an experimental, pressure-controlled extrusion 3D printer (NOVA, Voltera, Kitchener, ON, Canada) with optical alignment and surface mapping. With a 500 µm

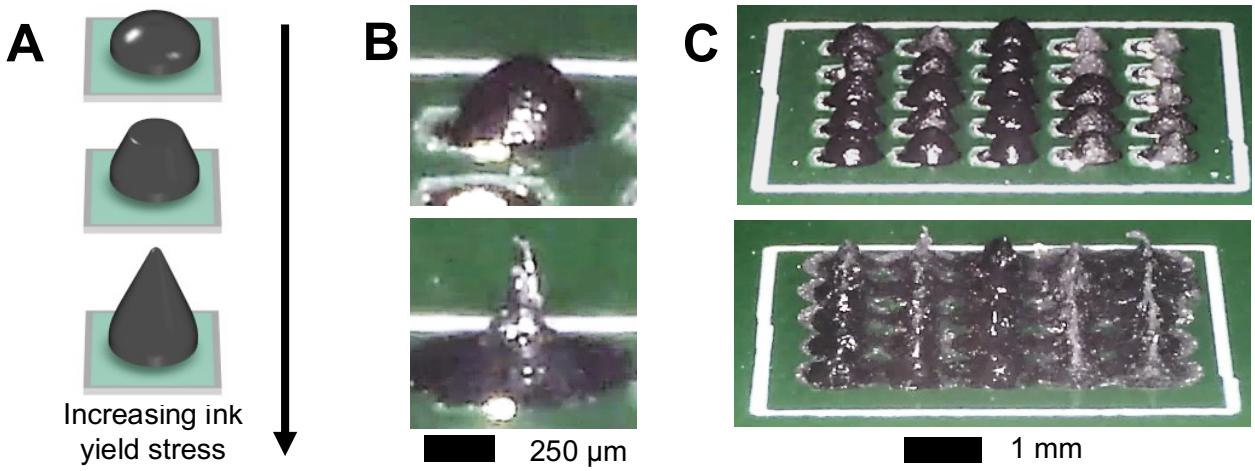

Figure 2: Effects of ink modulation. A) Schematic showing individual emitter geometry as affected by ink yield stress. B-C) Optical photographs of FEAs as affected by ink yield stress variation (top row 250 Pa, bottom row 610 Pa).

diameter nozzle tip, we created arrays of free-standing conical emitters (384 µm ± 69 µm tall, 65 µm ± 3 µm tip diameter). The process was tuned to attain narrow tip diameter with protruding surface-level CNTs and a large-area contact with the PCB surface to benefit electrical and thermal conduction, resulting in conical shapes.

CNT Ink Preparation

The deposited ink was tailored to fulfill competing specifications to create solid conical structures by extrusion of an ink with a high loading of CNTs and fine feature resolution. The resulting custom inks contain 13-15 wt% CNTs (CheapTubes, Grafton, VT, USA), 10-20 nm diameter, 0.5-2.0 µm in length, in an aqueous dispersion stabilized by 15-17 wt% sodium deoxycholate (DOC) surfactant and were prepared by gradual addition of a mixture of the dry CNTs and DOC to water followed by tip sonication at low power (XL-2020, Misonix, Farmingdale, NY, USA, power "2") for 30 minutes until smooth. Finally, a small amount of pre-formulated ink with single-walled CNTs were added (0.10-0.15% final mass fraction in the ink; Coat_E, OCSiAl, Luxembourg) to improve solution ductility. This method builds on previous methods of ink production, using an understanding of the scalings of CNT-based rheology to tailor the formulations [9].

To avoid chemical curing or sintering steps, these concentrated inks were optimized to have moderate-to-high shear yield stresses at rest. Yield stress behavior mechanically enables the printing of objects with good feature fidelity [12]. For a field emission application, the presence of a yield stress also facilitates the formation of sharp, centered peaks during detachment of the ink from the printing nozzle due to the fluid filament breakup [13] (shown schematically in Figure 1b). After ink deposition, the yield stress counteracts gravity and Laplace pressure from the surface tension of the ink solvent to preserve printed tip features in stable form [10]. We compared printed arrays made from two inks with yield stresses of 250 and 610 Pa respectively having 13 and 15 wt% CNTs, to assess the impact on resolution resulting from small variations in ink production. Sub-100 µm tips (Figure 2) were extruded with the 500 µm nozzle. The high-concentration ink was used for the remaining study. Further, all inks exhibited shear-thinning rheology, allowing extrusion from fine nozzles despite high stresses exhibited at rest. The printed CNT ink had a material cost of $6.63 per mL, or $0.00066 per emitter ($10^{-4}$ mL volume).

After printing, the solvent was removed by evaporation in ambient conditions. The high CNT content prevented excessive shrinkage during drying, though a similar yield stress could have been achieved with a smaller concentration of longer CNTs [14]. Inks with higher CNT concentration (18 wt%) could be produced but could not be extruded without clogging. Altogether, the novel ink formulation facilitated the printing of short, freestanding structures (Figure 3), requiring neither polymeric fillers that reduce electrical conductivity of the emitters, nor a curing step that could hinder PCB process compatibility.

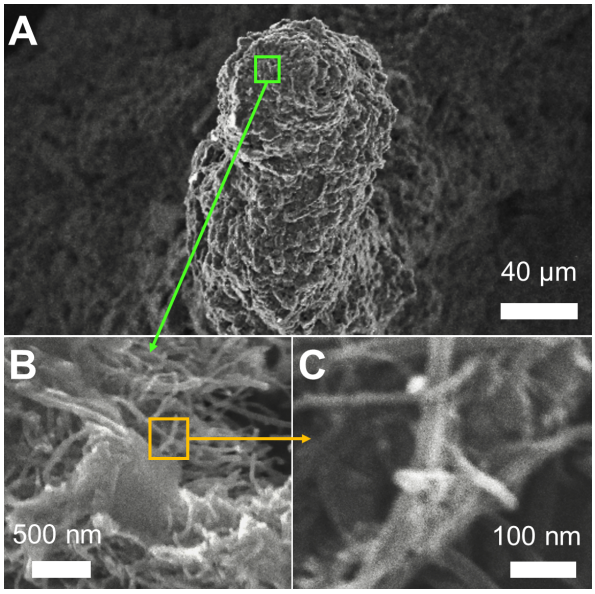

Figure 3: Scanning electron micrograph (SEM) views of a 3D-printed emitter. A) Overhead view, showing an as-printed tip diameter of ~65 µm, with far finer features derived from the CNT ink. B-C) CNT bundles protruding from emitter. The effective emission length scale from Fowler-Nordheim analysis is 4-7 nm per emitter, visually corresponding to protrusions on the multi-walled CNTs viewed in C.

RESULTS

Electrical characterization in 10^{-6} Torr vacuum of the 3D-printed FEAs in diode configuration (emitters, counter electrode) used a duo of Keithley 2657a power supplies (Keithley Instruments, Cleveland OH, USA). Emission results show a turn-on electric field of 0.1 V/µm, max current density of 1 mA/ cm^2, 10 µA total emission current at 1 V/µm, and field enhancement factor $\beta \approx 1 \times 10^5$ cm^{-1} (Figure 4), in line with previously demonstrated results for CNT-based emitters [4]. Results are consistent for the full array and for two example individually addressed units, one on the array edge and one in the array center. Data follow the Fowler-Nordheim (FN) model [11], and standard FN analysis of the least-squares fitting of the data indicates that the emitters have 4-7 nm quantum tunneling features, potentially corresponding to single CNTs or portions of CNT sidewalls emitting from the top surfaces of the printed structures.

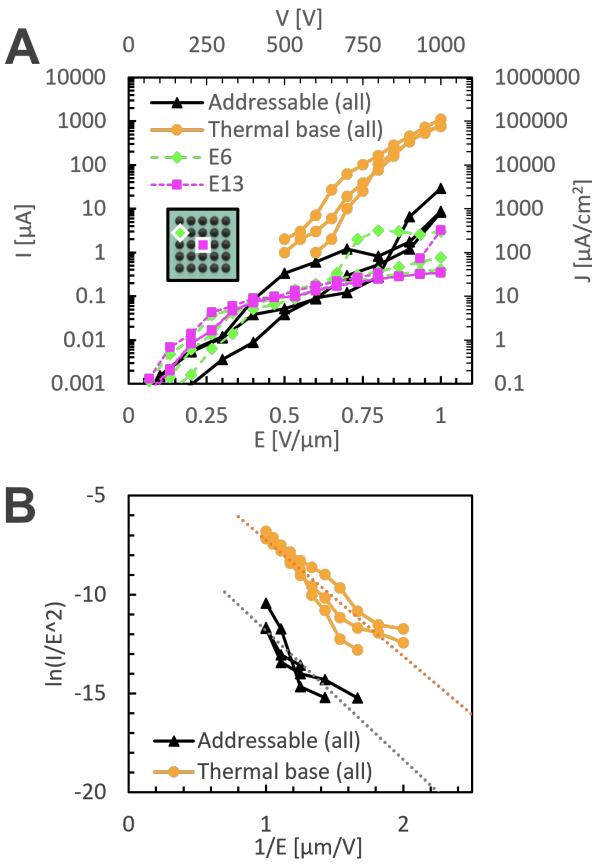

Figure 4: Emission data from an individually addressable FEA ("Addressable") activated in bulk and a variant printed on a bulk copper substrate for heat dissipation ("Thermal base"). A) Direct emission current (left axis) and array current density (right axis) vs. nominal electric field strength (bottom axis) and applied bias voltage (top axis) for both bulk activation tests and for representative activations of two individual emitters, whose locations in the array are marked by colored shapes (inset). Data are shown for three voltage sweeping cycles per sample. B) Fowler-Nordheim plot for both bulk activation tests, from which field enhancement factors and activation areas were computed. Dotted lines show linear fits of $ln(I/E^2)$ vs 1/E; a linear fit implies Fowler-Nordheim model conformity.

Characterization of arrays of individually addressed emitters shows that the total emitted current scales with the number of emitters; individual emitters have a turn-on field of 0.1 V/µm, ~0.4 µA emission current at 1 V/µm, and $\beta \approx 4 \times 10^5$ cm^{-1} field enhancement factor. The same FEA structures printed onto a monolithic copper electrode show improved properties, with a higher turn-on field (0.5 V/µm), peak array current density (>100 mA/cm^2), total emission current of 1000 µA at 1 V/µm, and similar field enhancement factor ($\beta \approx 2 \times 10^5$ cm^{-1}), possibly due to more efficient heat dissipation and power delivery through the copper base. Poole-Frenkel dielectric breakdown was excluded from possibility by testing the devices in reverse polarity; no emission was observed when the bias voltage acting on the emitters was above the bias voltage of the counter electrode.

DISCUSSION

The FEAs reported here demonstrate the potential to directly 3D print individually addressable field emission electron sources onto functional devices in an automated process. Benefitting from the compatibility of additive manufacturing with a variety of substrates, the proposed cathode technology has excellent relevance to industrial challenges. The reported devices meet state-of-the-art performance for CNT-based field emitters [3],[4] while enabling individual emitter addressability. This combination of features is a critical requirement to enable field uniformity correction in EPL [5], without which distortion of projected patterns occurs. Recorded performance herein immediately satisfies the expected emission current density of 10-600 µA/cm^2 for a commercial EPL system.

Further, the customizable deposition of emitters on arbitrary substrates has great utility for medical imaging, as integration with existing infrastructure can allow products to incorporate CNT inks directly. Controllable emission localization also enables high-precision X-ray imaging via phase contrast signal encoding in the emission pattern [8].

While existing cleanroom-made FEAs have excellent performance [14],[16], their cost of iteration and integration difficulty lead to 3D printing being a more sustainable approach for limited-scale production. Here, the cost of printing hardware is under $100,000, while total device fabrication time (including setup and calibration) is under 5 minutes. This enables vastly expedited development timeframes without continuing expenses associated with cleanroom usage.

No byproduct waste is produced during the printing process for the FEAs reported here besides residual ink, avoiding significant quantities of environmental pollutants and toxins released during subtractive processing of conventional devices, often made via etching in cleanroom lithography protocols. Most costs associated with hazard disposal are thus avoided.

Ongoing efforts focus on increasing emitter array density while sustaining the same per-emitter current, with a view towards leveraging other benefits of additive manufacturing (e.g., topological customization or use of

non-planar base substrates) for obtaining new emission modalities. With additional process and ink refinement, emitter dimensions can become more precise, allowing for smaller-scale emitters and consequently higher packing density. More tailored manufacturing such as parallel dispensing [17] could create large-scale arrays, further reducing FEA fabrication costs and heralding the next generation of vacuum electron sources.

ACKNOWLEDGEMENTS

This work was sponsored in part by the NewSat project. The NewSat project is co-funded by the Operational Program for Competitiveness and Internationalisation (COMPETE2020), Portugal 2020, the European Regional Development Fund (ERDF), and the Portuguese Foundation for Science and Technology (FTC) under the MIT Portugal program. Project support was also received from the Soft Matter Group within the Materials and Manufacturing Directorate of the Air Force Research Laboratory and from Lincoln Labs. C. E. Owens was supported by a MathWorks Engineering Fellowship from MIT. The authors would like to thank Voltera for assistance with the NOVA instrument, and Dr. Megan A. Creighton for advice in formulating the carbon nanotube ink.

REFERENCES

[1] L. F. Velásquez-García, B. Gassend, and A. I. Akinwande, "CNT-based MEMS ionizers for portable mass spectrometry applications," *J. Microelectromech. Syst.* vol. 19, no. 3, pp. 484 – 493, June 2010, doi: 10.1109/JMEMS.2010.2045639

[2] A. A. Fomani, A. I. Akinwande, and L. F. Velásquez-García, "Resilient, nanostructured, high-current, and low-voltage neutralizers for electric propulsion of small spacecraft in Low Earth Orbit," *Journal of Physics: Conference Series* vol. 476 (2013) 012014, doi: 10.1088/1742-6596/476/1/012014

[3] S. B. Fairchild *et al.*, "Carbon nanotube fiber field emission array cathodes," *IEEE Trans. Plasma Sci.*, vol. 47, no. 5, pp. 2032–2038, May 2019, doi: 10.1109/TPS.2019.2900219

[4] C. E. Owens *et al.*, "Pointwise fabrication and fluidic shaping of carbon nanotube field emitters," in *2021 21st International Conference on Solid-State Sensors, Actuators and Microsystems (Transducers)*, Orlando, FL, USA, Jun. 2021, pp. 912–915. doi: 10.1109/Transducers50396.2021.9495415

[5] M. Esashi, A. Kojima, N. Ikegami, H. Miyaguchi, and N. Koshida, "Development of massively parallel electron beam direct write lithography using active-matrix nanocrystalline-silicon electron emitter arrays," *Microsyst Nanoeng*, vol. 1, no. 1, p. 15029, Dec. 2015, doi: 10.1038/micronano.2015.29

[6] I. A. Perales-Martinez and L. F. Velásquez-García, "Fully 3D-printed carbon nanotube field emission electron sources with in-plane gate electrode," *Nanotechnology*, vol. 30, no. 49, p. 495303, Dec. 2019, doi: 10.1088/1361-6528/ab3d17

[7] A. Kachkine and L. F. Velásquez-García, "Densely packed, additively manufactured, in-plane gated carbon nanotube field emission electron sources," in *2022 21st International Conference on Micro and Nanotechnology for Power Generation and Energy Conversion Applications (PowerMEMS)*, Dec. 2022, pp. 38–41. doi: 10.1109/PowerMEMS56853.2022.10007579

[8] R. Gupta, L. F. Velasquez-Garcia, R. Lanza, B. K. Horn, and T. Akinwande, "Method for coded-source phase contrast x-ray imaging," WO2013187970A2, Dec. 19, 2013.

[9] C. E. Owens *et al.*, "Substrate-versatile direct-write printing of carbon nanotube-based flexible conductors, circuits, and sensors," *Adv. Func. Mat.*, vol. 31 (25) 2100245, 2021. doi: 10.1002/adfm.202100245.

[10] A. M'Barki, L. Bocquet, and A. Stevenson, "Linking rheology and printability for dense and strong ceramics by direct ink writing," *Sci Rep*, vol. 7, no. 1, Art. no. 1, Jul. 2017, doi: 10.1038/s41598-017-06115-0.

[11] R. G. Forbes, "Development of a simple quantitative test for lack of field emission orthodoxy," *Proceedings of the Royal Society A: Mathematical, Physical and Engineering Sciences*, vol. 469, no. 2158, p. 20130271, Oct. 2013, doi: 10.1098/rspa.2013.0271.

[12] M. Milazzo *et al.*, "3D Printability of Silk/hydroxyapatite composites for microprosthetic applications," *ACS Biomater Sci Eng*, vol. 9, no. 3, pp. 1285–1295, Mar. 2023, doi: 10.1021/acsbiomaterials.2c01357.

[13] Q. Barral, G. Ovarlez, X. Chateau, J. Boujlel, B. Rabideau, and P. Coussot, "Adhesion of yield stress fluids," *Soft Matter*, vol. 6, no. 6, pp. 1343–1351, Mar. 2010, doi: 10.1039/B922162J.

[14] S. S. Rahatekar, *et al.*, "Length-dependent mechanics of carbon nanotube networks," *Adv Mat*, 21, 2009. doi: 10.1002/adma.200802670

[15] S. Cheng, F. A. Hill, E. V. Heubel, and L. F. Velásquez- García, "Low-bremsstrahlung X-ray source using a low-Voltage high-current-density nanostructured field emission cathode and a transmission anode for markerless soft tissue imaging," *J. Microelectromech. Syst.,* vol. 24, no. 2, pp. 373 – 383, April 2015, doi: 10.1109/JMEMS.2014.2332176

[16] A. Basu, M. E. Swanwick, A. A. Fomani, and L. F. Velásquez-García, "A portable X-ray source with a nanostructured Pt-coated silicon field emission cathode for absorption imaging of low-Z materials," *J. Phys. D – Appl. Phys.* vol. 48, no. 22, 225501, May 2015, doi: 10.1088/0022-3727/48/22/225501

[17] S. G. M. U, *et al.*, "Multimaterial multinozzle adaptive 3d printing of soft materials," *Adv. Mat. Tech.*, vol. 7 (8) 2101710, 2022. doi: 10.1002/admt.202101710

CONTACT

*C. E. Owens, crystalo@mit.edu
*A. Kachkine, kashkin@mit.edu
*G. H. McKinley, gareth@mit.edu
*L. F. Velásquez-García, Velasquez@alum.mit.edu
*A. J. Hart, ajhart@mit.edu